AIChE

Electric Conductance Method to Study the Contact of Injected Liquid with Fluidized Particles

Federica Portoghese, Peter House, Franco Berruti, and Cedric Briens
Dept. of Chemical and Biochemical Engineering, The University of Western Ontario, London, ON, Canada N6A 5B9

Kazimierz Adamiak
Dept. of Electrical and Computer Engineering, The University of Western Ontario, London, ON, Canada N6A 5B9

Edward Chan
Syncrude Canada, Ltd., Edmonton Research Center, Edmonton, AB, Canada T6N 1H4

DOI 10.1002/aic.11500
Published online May 29, 2008 in Wiley InterScience (www.interscience.wiley.com).

A sensitive and reliable experimental technique was developed to assess the performance of gas-atomization nozzles injecting liquid into a gas-solid fluidized bed. Gas atomizers are used to inject liquid feeds into industrial fluid cokers, fluid catalytic crackers, and gas-phase polymerization reactors. In the fluid coking process, for example, both liquid yields and reactor operability are affected by how well the injected liquid contacts the fluidized particles. The new experimental method assesses the quality of the liquid-solid contact from the electric conductance of the bed solids wetted with the injected liquid. The validity of the method was corroborated by direct comparison with the results provided by alternative experimental techniques, as well as by numerical modeling of the evolution of the bed conductance for various types of liquid distribution within the bed solids. The electric conductance technique can help optimize liquid injection into fluidized beds. © 2008 American Institute of Chemical Engineers *AIChE J,* 54: 1770–1781, 2008

Keywords: gas-liquid jets, gas-solid fluidized bed, fluid coking, spray nozzle, liquid injection

Introduction

In numerous industrial applications, liquid is injected into fluidized-bed reactors. In the petroleum industry, for example, bitumen and heavy oils are upgraded by cracking the liquid feed on hot fluidized solid particles. In industrial fluid cokers, bitumen is injected into the reactor via steam-assisted nozzles where it contacts fluidized coke particles preheated at a temperature ranging from 500 to 550 °C. The hot coke particles provide the heat required for the endothermic thermal cracking of the bitumen molecules to lighter products. Both the hydrocarbon conversion efficiency and the operability of the reactor are strongly affected by the initial contact between the injected liquid and the fluidized solids.[1,2] It has been shown that improving the contact of injected liquid with fluidized particles increases the yield of valuable liquid products in both the fluid catalytic cracking process, where most of the liquid is vaporizable, and in the fluid coking process, where most of the liquid is not directly vaporizable, but must first be cracked to generate vaporizable fractions.[1,3] In the case of vaporizable liquids, liquid-solid agglomerates may or may not be formed, depending on the operating conditions,[4,5] while they always form with nonvaporizable liquids.[6] Bruhns et al.[7] investigated the interaction between vaporizable liquid jets and fluidized solids in a pilot-scale re-

Correspondence concerning this article should be addressed to C. Briens at cbriens@uwo.ca.

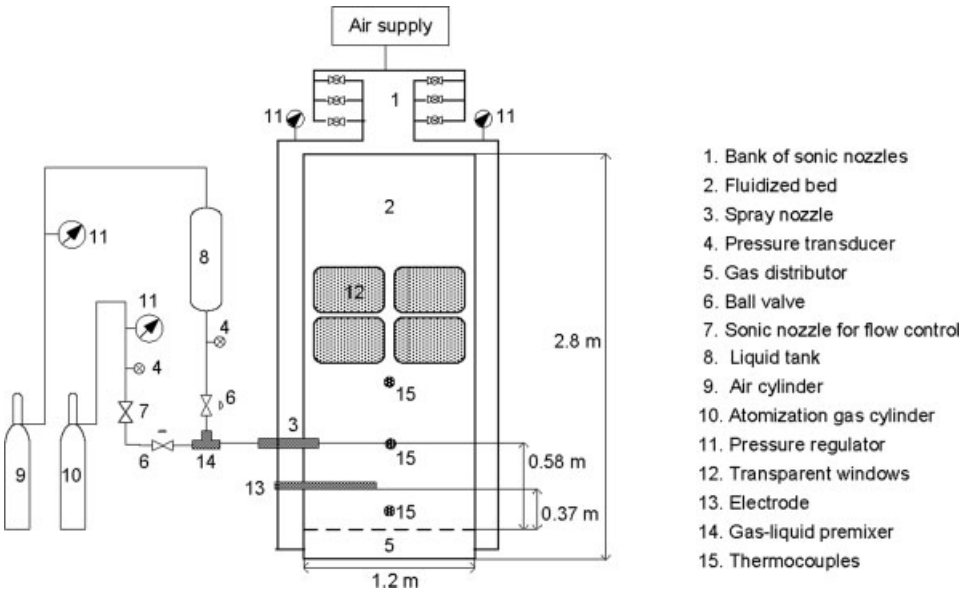

Figure 1. Fluidized-bed apparatus and liquid-injection setup.

actor operated at 120–180 °C. Their study indicated that the liquid injected through commercial gas-atomization nozzles did not immediately vaporize upon direct contact with the bed solids. Instead, liquid-solid agglomerates were formed in the proximity of the spray nozzle, from where they were transported into the interior of the reactor. The same behavior was observed using either water or ethanol with both FCC and sand particles.

With nonvaporizable liquids, using an X-ray imaging technique, Ariyapadi et al.[6] visually observed the formation of liquid-solid agglomerates at the tip of the cavity formed by the liquid jet in a laboratory-scale fluidized bed of coke particles. The formation of agglomerates upon the contact between liquid jets and a small-scale fluidized bed was quantified by House et al.[1,8] They injected a binder solution via gas-atomization nozzles into a fluidized bed of coke particles at room-temperature, and froze the formed agglomerates right after completing the liquid injection by interrupting the fluidization air. They found that both the nozzle internal geometry and internals, such as a draft tube or an impact cone interacting with the liquid jet, have a strong impact on the quality of the liquid-solid contact. This was confirmed in a fluid coking pilot plant by Knapper et al.[9] who compared the spraying efficiency of two feed nozzles having a different internal geometry. Their study showed that, while the coating efficiency of solids with liquid was nearly double with the higher performance nozzle, for both cases only a small fraction of the solid particles could be contacted by liquid. This finding strengthens the importance of directing further research toward the improvement of conventional liquid-injection technologies.

The objective of this study was to develop an experimental technique for assessing the spraying performance of nozzles injecting liquid into a fluidized bed. In a previous work by the authors,[10] a technique based on triboelectric measurements was presented. The triboelectric technique is rapid and can be easily scaledup to evaluate the relative performance of commercial-scale spray nozzles. A limitation of the triboelectric technique is that, since it measures a current generated by collisions of bed particles with an electrode, it is very sensitive to the local bed hydrodynamics. The main objective of this article was to develop a different method that would be much less sensitive to the local bed hydrodynamics. This article presents a different technique, which is based on measuring the electrical conductance of the bed solids after completing the liquid injection and defluidizing the wetted particles. Mixing the solids with a liquid, having a higher electrical conductivity increases the overall bed electric conductance, as liquid is more uniformly mixed with solids. Therefore, a larger bed conductance indicates a more effective interaction of the liquid feed with the bed particles, i.e., a higher nozzle performance.

A numerical model was developed to analyze the effect of the liquid-solid mixing produced by the injection of liquid into the fluidized bed on the measured bed electrical conductance. Furthermore, a reaction model proposed by House et al.[11] which considers the effects of mass transfer, heat transfer and reaction kinetics on the coking of bitumen, was, then, used to predict the impact that the liquid distributions indicated by the conductance model would have on the progress of cracking reactions in a fluid coker.The conductance technique was applied to test the effect of the gas-to-liquid ratio on the spraying performance of gas-atomized liquid-injection nozzles. The experimental results obtained with the electric conductance method were successfully compared with those provided by the triboelectric method.

Experimental

Experimental setup and materials

Figure 1 illustrates the fluidized bed and the liquid-injection setup employed in this study. The cross-section of the fluidized bed is rectangular with dimensions 1.2 m by 0.15

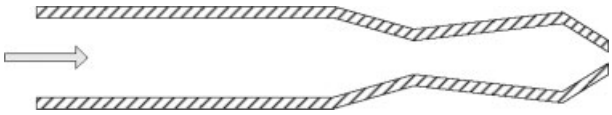

Figure 2. Geometrical configuration of the spray nozzle.

m. The bed was operated with 246 kg of silica sand particles having an apparent particle density of 2,600 kg/m^3, and a Sauter-mean diameter of 190 μm, which corresponded to a static bed height of 0.85 m. The solids were air-fluidized at a superficial gas velocity of 0.24 m/s. An array of three thermocouples monitored the average bed temperature to ensure a constant value of 20°C prior to every liquid injection. The relative humidity of the fluidization air was maintained at 12–13%.

The liquid-injection system was comprised of an air-atomization spray nozzle horizontally inserted into the bed about 0.6 m above the air distributor, an air-liquid premixer located upstream of the nozzle, and the liquid and atomization-air lines. For all the experiments, the injected liquid was deionized water. The air-mass flow rate was adjusted by regulating the gas pressure upstream of calibrated sonic nozzles. For any required gas flow rate, the water flow rate was regulated by adjusting the pressure of a water tank connected to a high-pressure cylinder. All water injections were performed at a constant flow rate of 22 g/s. The air flow rate was adjusted to yield gas-to-liquid mass ratios (ALR) in the range between 0 and 3.3 wt %. The internal geometry of the gas-assisted spray nozzle is schematically depicted in Figure 2. The design of the nozzle has been patented for industrial fluid coking operations.[12]

Measurements of the bed electrical conductance

The stainless-steel walls of the fluidized bed, as well as the air distributor were electrically grounded. As shown in Figure 1, an electrode was horizontally installed in the bed at a distance of approximately 0.37 m from the air distributor. Teflon fittings were used to provide electrical insulation between the electrode and the bed wall. The electrode consisted of a stainless-steel hollow tube soldered at both extremities, and having an outer diameter of 0.01 m. It penetrated into the bed for a length of 0.65 m.A signal generator was used to apply an AC voltage between a measurement resistor (R_m) connected in series with the electrode, and the ground, as indicated in Figure 3.

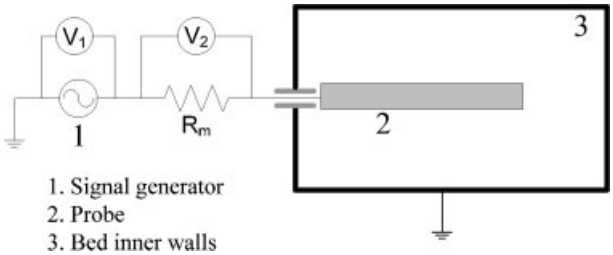

Figure 3. Electric conductance measurements.

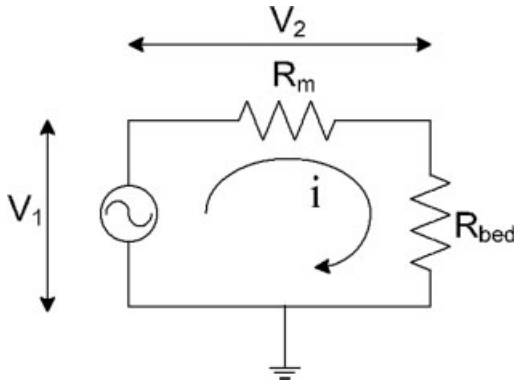

Figure 4. Equivalent electric circuit for electric conductance measurements.

The voltages across both the signal generator (V_1), and the measurement resistor (V_2) were measured at a rate of 1,200 Hz. The RMS value of the generated voltage V_1, was 6.7 V, and its frequency was equal to 60 Hz. Figure 4 shows the equivalent circuit of the measurement system. Applying a voltage across the series of measurement resistor, electrode, and bed material produces an electric current flowing between the electrode and the bed walls (I). For a given applied voltage (V_1), and a given measurement resistance (R_m), both the amplitude and the phase of the alternating current depend on the electric behavior of the bed material interposed between the electrode and the grounded bed walls.

Preliminary tests indicated that when dry bed solids are defluidized, the electric current flowing through the settled particles is in phase with the applied voltage. The same result was observed when the bed solids were defluidized after injection of a more electrically conductive liquid into the bed, suggesting that, either dry or wetted with a more conductive liquid, the packed solids do not exhibit any capacitive or inductive effect. Furthermore, they were found to obey Ohm's law, i.e., the relationship between the applied voltage and the measured electric current was linear for several tested values of V_1. The electric behavior of the defluidized bed solids was, thus, described in terms of the bed resistance (R_{bed}) or, equivalently, its inverse, the bed conductance (C_{bed}). For a given value of R_m, the bed resistance can be estimated by means of Eq. 1

$$R_{\text{bed}} = \left(\frac{V_1}{V_2} - 1\right) R_m \tag{1}$$

Liquid injections via gas-atomization nozzle

Every liquid injection was carried out for 15 s while maintaining fluidization conditions. The fluidization air was shut down 2 s after the end of the liquid injection, allowing the wetted bed solids to defluidize. The resistance of the fixed bed was continuously measured for about 400 s. After completing the measurements, the fluidization air was turned on to evaporate the liquid. Due to evaporative cooling of the particles, about 30 min of continuous fluidization were required to return to the selected average bed temperature of 20 °C.

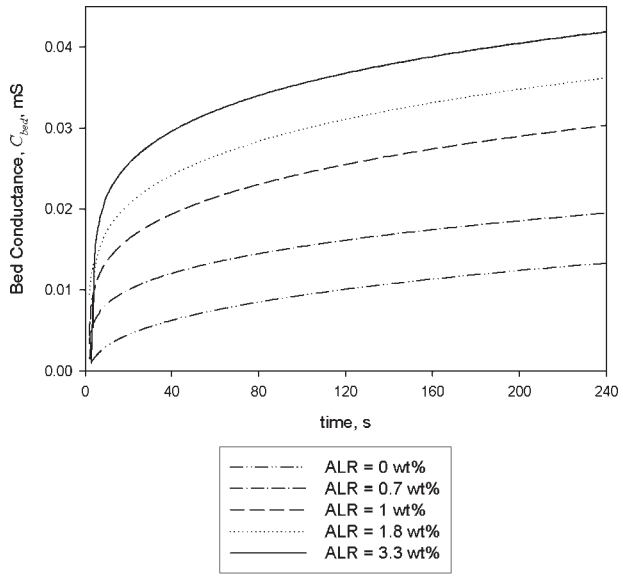

Figure 5. Measured bed conductance C_{bed}, vs. time t, for various air-to-liquid ratios, ALRs.

The liquid injection was completed at $t = 0$. The bed was defluidized at $t = 2$ s.

Figure 5 shows the time evolution of the bed electric conductance resulting from liquid injections carried out with five different values of the air-to-liquid ratio (ALR) within the range between 0 and 3.3 wt %. A few seconds were required for the bed material to settle after the fluidization gas supply was shut down. After bed defluidization, the bed conductance increased with time for all of the performed liquid injections. Such increase in the bed conductance was produced by the gradual spreading of the injected water over the settled particles due to capillary forces. Moreover, Figure 5 shows that increasing the ALR resulted in consistently higher-bed conductance. For example, about 10 s after the shutting off the fluidization gas, the bed conductance corresponding to the injection with an ALR of 3.3 wt % was approximately nine times higher than that produced by the liquid-only injection (ALR = 0 wt %). The bed particles belonged to Geldart's group B and defluidized very quickly. Visual observations through windows running over the whole bed length confirmed that, 10 s after shutting off the fluidization gas, the bed surface remained perfectly still.

Previous experimental work by the authors[13,14] indicated that higher ALRs provide a more effective atomization of the injected liquid, which in turn produces a more uniform distribution of the liquid on the bed particles. It was, therefore, assumed that the more effective coating of the particles with the electrically conductive liquid was responsible for the larger overall bed conductance achieved at higher ALR.

External premixing experiment

The validity of this interpretation was partially confirmed by an *external premixing experiment*, which followed the procedure presented in Portoghese et al.[10] Instead of injecting the liquid via the air-atomization nozzle, known amounts of water and bed solids were first uniformly premixed in a rotating drum, and then introduced into the bed through the windows shown in Figure 1. The wetted solids were fluidized with the rest of the bed particles, which were dry, at a fluidization velocity of 0.24 m/s for about 80 s, after which the bed was defluidized to measure the conductance of the wetted bed solids. Assuming that the fluidization air was fully saturated with water vapor (relative humidity of 100%), the rate of water evaporation was calculated from the measured average bed temperature at any time instant during fluidization. For a few preliminary tests, the mass of water premixed with the solids in the rotating drum was adjusted so that the overall bed liquid-to-solid ratio (L/S) after 80 s of fluidization was the same as for the liquid injections via nozzle (L/S = 0.134 wt %).

Figure 6 shows that the bed conductance corresponding to the *external premixing experiment* very quickly stabilized at an approximately constant value, confirming that nearly ideal spreading of the liquid on the particles had been achieved. The bed conductance was also significantly higher than the conductance obtained with all the nozzle injections at any time after the bed defluidization ($t = 0$ s) (Figure 5). This result is in agreement with the finding by the authors[10] that premixing a fraction of the bed solids with liquid in a mixing device, such as a rotating drum provides a more effective coating of solid particles with liquid than injecting the liquid directly into the fluidized bed with a spray nozzle.

Modeling the bed conductance

The modeling activity was aimed at providing further insight into the relationship existing between the bed electric conductance and the quality of the liquid distribution on the bed solids.

The spreading of the injected water on the packed-bed solids, and the resulting time evolution of the overall bed electric conductance were modeled using a commercial software (COMSOL Multiphysics 3.2). The finite element method (FEM) was used to numerically solve the partial differential equations governing the diffusion of water throughout the bed solids, and its effect on the electric field established between the electrode and the bed walls and air distributor.

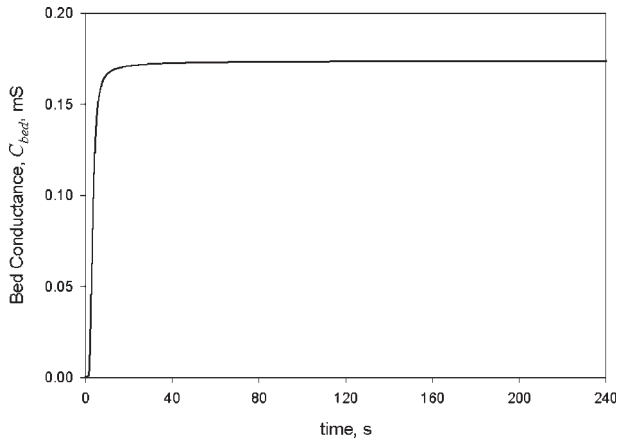

Figure 6. Measured-bed conductance C_{bed} vs. time t, for the external premixing run.

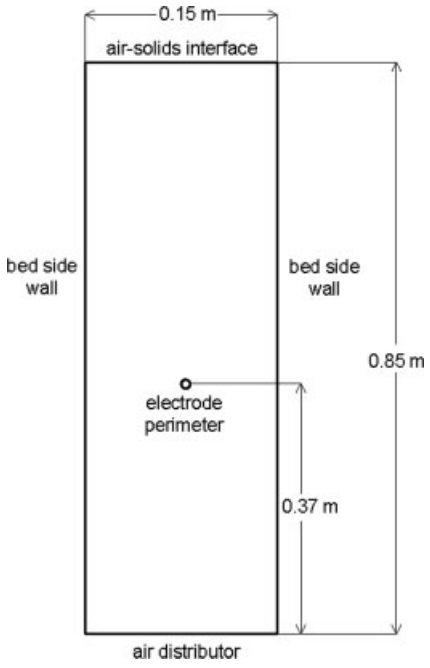

Figure 7. Computational domain used for FEM modeling.

The computational domain was restricted to a cross-section of the bed solids perpendicular to the longitudinal axis of the electrode (Figure 7).

As shown in Figure 7, the domain boundaries consisted of two of the bed side walls, the air distributor at the bottom, the solids free surface area at the top, and the outer perimeter of the probe.

The domain was discretized using an unstructured mesh of triangular finite elements. For each element, the dependent variables were approximated using piecewise polynomials of order three. A direct linear system solver (UMFPACK) was used to solve the discretized partial differential equations.

Initialization of the domain with given liquid distribution in the fixed bed

The first computational step was the initialization of the domain with the liquid concentration field corresponding to the assumed liquid distribution at the time when the bed was defluidized. To this purpose, it was assumed that only a fraction of the injected liquid could mix uniformly with the particles, whereas the rest of the liquid formed liquid-solid blobs of larger wetness. As a further simplifying assumption, all the liquid-solid blobs were considered to have the same water content, or liquid-to-solid weight ratio

$$L/S_{\text{blob}} = \frac{M_{\text{Lblob}}}{M_{\text{Sblob}}} = \frac{\rho_L}{\rho_S}\frac{V_{\text{Lblob}}}{V_{Sblob}} \tag{2}$$

where ρ_L and ρ_S are the liquid and solids densities, M_{Lblob} and $M_{S\text{blob}}$ are the masses of liquid and solid confined within each blob, and V_{Lblob} and V_{Sblob} are the volumes occupied by the two phases in each blob. For the two-dimensional (2-D) geometry shown in Figure 7, the liquid-to-solid ratio of a blob can be expressed in terms of the surface areas S_{Lblob} and S_{Sblob}, occupied by the two phases within each circular blob of radius R_{blob}

$$L/S_{\text{blob}} = \frac{\rho_L}{\rho_S}\frac{S_{\text{Lblob}}}{S_{\text{Sblob}}} \tag{3}$$

Considering that only a fraction of the injected liquid is segregated within blobs (M_{Lsegr}), the rest being uniformly mixed with the particles (M_{Lfree}), the total liquid-to-solid ratio can be split up into two separate contributions as given in Eq. 4

$$L/S_{\text{total}} = \frac{M_{\text{Ltotal}}}{M_{\text{Stotal}}} = \frac{M_{\text{Lsegr}}}{M_{\text{Stotal}}} + \frac{M_{\text{Lfree}}}{M_{\text{Stotal}}} = f_{\text{segr}} + f_{\text{free}} \tag{4}$$

where M_{Ltotal} and M_{Stotal} are the total masses of liquid and solid in the entire domain, f_{segr} is the ratio of M_{Lsegr} to the total mass of solids, and f_{free} is the ratio of M_{Lfree} to the total mass of solids. The fraction of liquid forming blobs (x_{blobs}) is defined in Eq. 5

$$x_{\text{blobs}} = \frac{M_{\text{Lsegr}}}{M_{\text{Ltotal}}} \tag{5}$$

The fraction of liquid forming blobs can be related to the total number of blobs N_{blob}, and the mass of uniformly wetted solids outside of the blobs M_{Sfree}

$$x_{\text{blobs}} = \frac{f_{\text{segr}}}{L/S_{\text{total}}} = \frac{N_{\text{blob}}M_{\text{Lblob}}}{N_{\text{blob}}M_{\text{Sblob}} + M_{\text{Sfree}}} \cdot \frac{1}{L/S_{\text{total}}} = \frac{N_{\text{blob}}L/S_{\text{blob}}}{N_{\text{blob}} + \frac{M_{\text{Sfree}}}{M_{\text{Sblob}}}} \cdot \frac{1}{L/S_{\text{total}}} \tag{6}$$

Designating with S_{total} the total surface area of the computational domain, M_{Sfree} can be expressed as

$$M_{\text{Sfree}} = \rho_S[S_{\text{total}} - N_{\text{blob}}\pi {R_{\text{blob}}}^2] \tag{7}$$

Since

$$S_{\text{Lblob}} + S_{\text{Sblob}} = \pi {R_{\text{blob}}}^2 \tag{8}$$

and

$$\frac{S_{\text{Lblob}}}{S_{\text{Sblob}}} = \frac{\rho_S}{\rho_L}L/S_{\text{blob}} \tag{9}$$

then, M_{Sblob} can be expressed as a function of R_{blob} and L/S_{blob}

$$M_{\text{Sblob}} = \rho_S S_{\text{Sblob}} = \frac{\rho_S \pi {R_{\text{blob}}}^2}{1 + \frac{\rho_S}{\rho_L}L/S_{\text{blob}}} \tag{10}$$

Substituting Eq. 10 in Eq. 6 yields the following relationship among the number of blobs, the wetness of each individual blob (L/S_{blob}), the blob size (R_{blob}), and the fraction of liquid forming blobs (x_{blobs})

$$x_{\text{blobs}} = \frac{N_{\text{blob}}L/S_{\text{blob}}}{N_{\text{blob}} + (1 + \frac{\rho_S}{\rho_L}L/S_{\text{blob}})(\frac{S_{\text{total}}}{\pi {R_{\text{blob}}}^2} - N_{\text{blob}})} \cdot \frac{1}{L/S_{\text{total}}} \tag{11}$$

By knowing the total bed wetness (L/S_{total}), and assuming values for x_{blobs}, L/S_{blob}, and R_{blob}, Eq. 11 was solved for

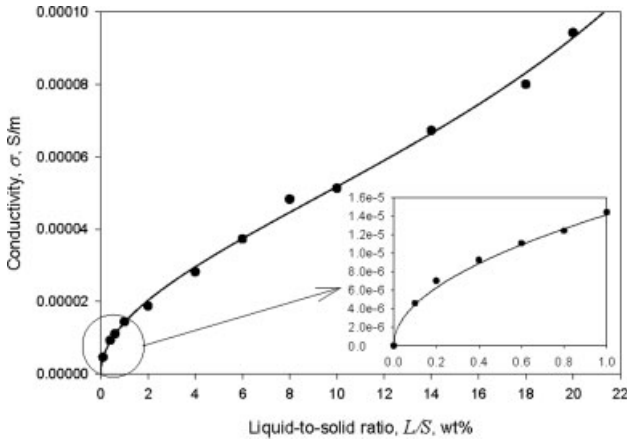

Figure 8. Experimentally determined correlation between the electric conductivity, σ, and the liquid-to-solid ratio *L/S*.

N_{blob}. In summary, the initial liquid distribution was uniquely determined by setting the values of three independent variables, namely the blob wetness (L/S_{blob}), the blob size (R_{blob}), and the fraction of liquid forming blobs (x_{blobs}).

The blobs were then randomly positioned within the bed cross-section by means of an auxiliary program using random number generators to define the spatial coordinates of the geometric center of each blob.

Modeling the diffusion of the liquid throughout the bed solids

The time-dependent spreading of water throughout the bed solids was described using a simplified macroscopic model with effective transport properties. The standard diffusion equation was used

$$\frac{\partial c}{\partial t} + \nabla \cdot (-D\nabla c) = 0 \tag{12}$$

In Eq. 12, c is the water concentration, t the time, and D the isotropic effective diffusion coefficient of water through the packed bed of sand particles. Neumann boundary conditions were imposed on all the domain boundaries by specifying a zero diffusion flux

$$\nabla c = 0 \tag{13}$$

Solution of Eqs. 12 and 13 yields the liquid concentration at any location within the fixed bed as a function of time and of the initial liquid distribution assumed $c = c\ (x, y, t)$.

Calculating the bed electrical conductance

The electric conductivity of the bed solids (σ) was measured using a conductivity cell coupled with an electrometer (602 Keithley Instruments) for various liquid-to-solid ratios ranging from 0 to 20 wt %, as shown in Figure 8. Replicates of the conductivity measurements for a few L/S values indicated reproducibility within $\pm$ 3.24 $\times$ 10^{-7} S/m.

At any time of interest, the electrical conductivity was calculated within the entire computational domain ($\sigma = \sigma\ (x, y, t)$) using the empirically determined correlation between σ and c.

Laplace's equation was then solved for the electric potential V

$$\nabla \cdot (\sigma \nabla V) = 0 \tag{14}$$

using Eqs. 15, 16 and 17 as the boundary conditions

$$\nabla V = 0 \ - \text{ electric insulation at the air-solids interface} \tag{15}$$

$$V = V_{ref} - \text{reference electric potential for the probe external perimeter} \tag{16}$$

$$V = 0 \ - \text{ ground potential for bed side walls and distributor} \tag{17}$$

Integrating the current density vector J, expressed in terms of the electric field E

$$J = \sigma E = -\sigma \nabla V \tag{18}$$

over the electrode perimeter provided the instantaneous value of the total electric current flowing between the electrode and the bed walls and distributor I

$$I = \oint J \cdot ndl \tag{19}$$

The overall electric conductance of the wetted solids (C_{bed}) was, hence, evaluated at any selected time as the ratio of the calculated total current I, to the potential difference between the electrode and bed walls, and the distributor V_{ref}

$$C_{bed} = \frac{I}{V_{ref}} \tag{20}$$

Evaluating the diffusion coefficient

Figure 9 illustrates the experimental apparatus used to evaluate the effective diffusion coefficient of the liquid throughout the packed solids. A box made of electrically insulating material was half filled with dry silica sand par-

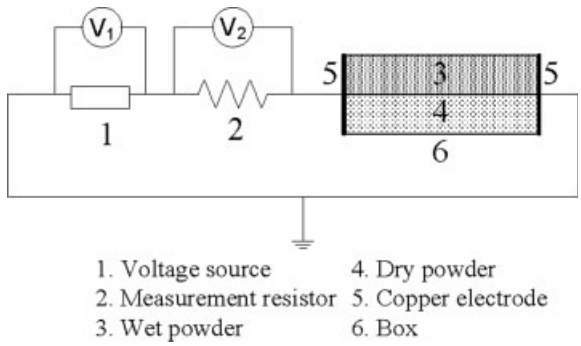

Figure 9. Setup used for measuring the diffusion coefficient in the box.

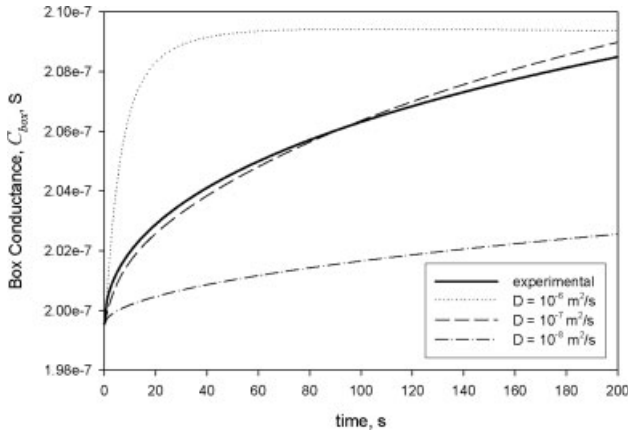

Figure 10. Comparison between the experimentally determined conductance of the box C_{box}, and the model predictions for three different values of the diffusion coefficient ($D = 10^{-6}$ m^2/s, 10^{-7}, and 10^{-8} m^2/s).

ticles, and half filled with particles that had been uniformly mixed with water (liquid-to-solid ratio of 20 wt %). A thin plate having the same longitudinal length as the box was interposed between the dry and the wet powder samples to prevent contamination before starting the measurement.

The box had a rectangular base of 0.044 m by 0.1 m, and a height of 0.02 m. The top surface was opened to the atmosphere. Two rectangular copper plates attached to the extremities of the box were used to apply a DC voltage across the wet and the dry powder samples. The voltage source was a 9-volt battery. The source voltage (V_1), and the voltage drop across the measurement resistor (V_2), were continuously measured using a data acquisition system. Measuring V_2 provided the electric current flowing through the box as the ratio of V_2 to the measurement resistance. The electrical conductance of the box (C_{box}) was calculated as the ratio of the current to the voltage drop across the box ($V_1 - V_2$). After the longitudinal plate separating the wet sample from the dry one had been removed, the gradual spreading of the water over the dry particles contacting the wetted sample increased the homogeneity of the whole liquid-solid mixture within the box, which in turn raised the box electrical conductance.

Figure 10 shows the progressive increase of the measured box conductance with time (experimental curve).

In order to evaluate the diffusion coefficient (D), several simulations of the change of the box conductance with time were conducted using various trial values for D. For each simulation, the procedure described in *Modeling the diffusion of the liquid throughout the bed solids* and *Calculating the bed electrical conductance* sections was adopted. Figure 10 shows the box conductance predicted for three different values of D, namely, 10^{-6} m^2/s, 10^{-7} m^2/s, and 10^{-8} m^2/s. It can be noted that the intermediate value of 10^{-7} m^2/s provided a satisfactory match with the measured conductance-vs. time curve over a range of liquid-to-solid ratio ranging from 0 to 20 wt %, and was therefore used for all the simulations described in the previous section.

Results and Discussion

Numerical results

A preliminary simulation of the electrical conductance of the dry bed was carried out using the measured electrical conductivity of the dry sand particles ($\sigma = 1.41 \times 10^{-11}$ S/m). The predicted value of the bed conductance (3.77×10^{-11} S) was found to be 7.9 times lower than that measured with the electrometer (2.98×10^{-10} S). Such discrepancy between the measured and the predicted values of the dry-bed conductance arises mostly from the intrinsic limitations of the 2-D geometry used in the simulations. While avoiding the overwhelming computational costs associated with 3-D simulations, the 2-D model geometry completely neglects the contribution of two of the bed-side walls to the electric field established within the bed, and, hence, leads to an underestimation of the bed conductance. Thus, a geometrical constant (F_g) was introduced to account for the geometrical differences existing between the 2-D model adopted and the real system. F_g was defined as the ratio of the measured to the predicted conductance of the dry bed

$$F_g = \frac{(C_{\text{bed}})_{\text{measured}}}{(C_{\text{bed}})_{\text{predicted}}} = 7.9 \tag{21}$$

Interestingly, correcting the predicted bed conductance for the limiting case of perfectly uniform liquid distribution (local L/S of 0.143 wt %) with the geometrical constant resulted in a value of 0.1817 mS, which is slightly higher than the pseudo-asymptotic value of the bed conductance measured during the *external premixing experiment* (0.1738 mS after 240 s from the bed defluidization). This suggests that, indeed, the *external premixing experiment* provided a nearly uniform mixing of the liquid with the solid particles.

Theoretically, the geometrical constant is valid only for perfectly homogeneous materials characterized by a uniform electrical conductivity (σ). Under these conditions, the overall conductance of a system (C) of given geometry can be expressed as

$$C = \sigma \cdot G \tag{22}$$

where G is the geometrical factor characteristic of the system. Equation 21 does not strictly apply to heterogeneous systems, such as a packed bed that is nonuniformly wetted with a liquid of different electric conductivity. However, provided the degree of homogeneity of the system be sufficiently high (pseudohomogeneous system), the error introduced by applying Eq. 21 is reasonably small. The validity of this assumption of pseudohomogeneity was tested by randomly changing the spatial location of the blobs within the 2-D geometry, and comparing the resulting conductance values. Only conductance values for which the variability associated with different blobs allocations was negligible were accepted. The conductance values predicted by these selected wet-bed simulations were multiplied by the geometrical constant defined for the dry bed.

Several simulations were conducted by separately changing each of the three independent variables characterizing the initial liquid distribution within the bed solids, namely, the

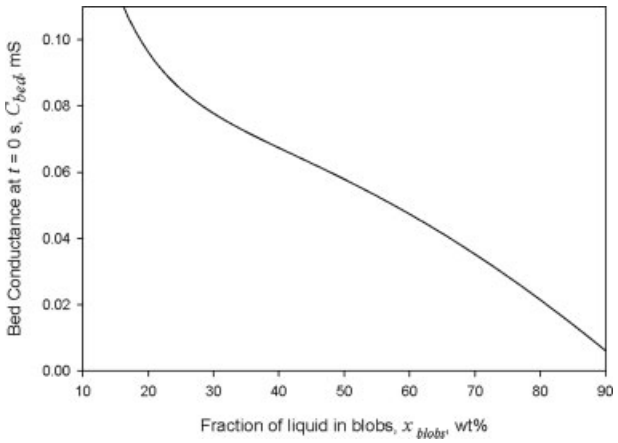

Figure 11. Predicted effect of the fraction of liquid in blobs, x_{blobs}, on the bed conductance (R_{blob} = 0.0025 m; L/S_{blob} = 0.4 wt %).

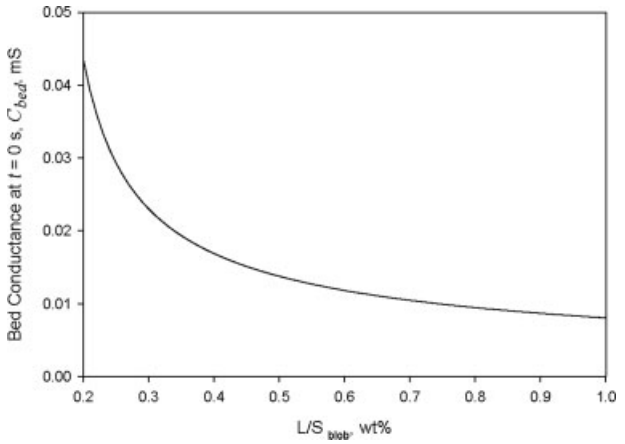

Figure 12. Predicted effect of L/S_{blob} on the bed conductance (R_{blob} = 0.0025 m; x_{blobs} = 84 wt %).

fraction of liquid forming blobs (x_{blobs}), the blob wetness (L/S_{blob}), and the blob size (R_{blob}). Such analysis allowed investigating the relative effect of each variable on the predicted bed electrical conductance. The diffusion of the liquid over time was not taken into account, and the simulations were carried out following the computational steps described in the *Initialization of the domain with given liquid distribution in the fixed bed* and *Calculating the bed electrical conductance* sections solely.

First, the fraction of liquid segregated within blobs (x_{blobs}) was varied between about 20 and 90 wt %, while keeping the liquid-to-solid ratio of each blob and the blob diameter constant and equal to 0.4 wt % and 5 mm, respectively. Figure 11 readily shows that the predicted bed conductance drops significantly as the fraction of liquid that segregates in the blobs is increased. This indicates that a more effective interaction between the liquid jet and the fluidized bed, leading to uniform mixing of a larger fraction of liquid with the solids would result in a higher bed conductance.

Second, the effect of the blob wetness on the bed conductance was explored by varying the liquid-to-solid ratio of the blobs between 0.2 and 1 wt %, and assuming the fraction of liquid in blobs equal to 84%, and the blob diameter equal to 5 mm. As shown in Figure 12, the predicted bed conductance decreases with increasing blob wetness. It was found that, for L/S_{blob} lower than 1 wt %, changes in the calculated bed conductance corresponding to different spatial locations of the blobs within the bed are negligible (pseudo-homogeneous system). On the other hand, for L/S_{blob} higher than 1–2 wt %, the number of blobs progressively decreases to values of a few hundreds or less for which the predicted bed conductance starts being affected by the blobs location within the bed (heterogeneous system). Limiting the maximum value of L/S_{blob} to 1 wt % ensured that the calculated bed conductance be independent of the blobs distribution throughout the 2-D computational domain. Figure 12 indicates that a better liquid injection producing more and drier blobs results in a higher bed conductance compared with a less effective injection of liquid forming a smaller number of wetter blobs.

Figure 13 shows how increasing the blob diameter from 5 to 8 mm produced a gradual decrease in the predicted bed conductance for all the tested L/S_{blob} of 0.4, 0.6, and 0.8 wt %. For all the simulations, the assumed fraction of liquid in blobs was 84%. Visual observations of the liquid-solid agglomerates laying on the bed-free surface through the transparent windows shown in Figure 1 indicated the maximum size of the formed agglomerates be less than 1 cm. Theoretically, any blob size between that of a cluster of a few particles and the observed size of 1 cm would be realistic. Simulating blobs smaller than 5 mm in diameter, however, would have required a much higher mesh resolution than that affordable with the available computational power. For this reason, all the simulations were restricted to blob diameters in the range between 5 and 8 mm.

Figure 13 indicates that enhancing the uniformity of the liquid distribution within the bed solids by producing a larger number of smaller agglomerates as opposed to a smaller number of bigger agglomerates results in a higher bed electrical conductance. This effect, however, is more pronounced at higher L/S_{blob}. For blob wetness as low as 0.4 wt %, the

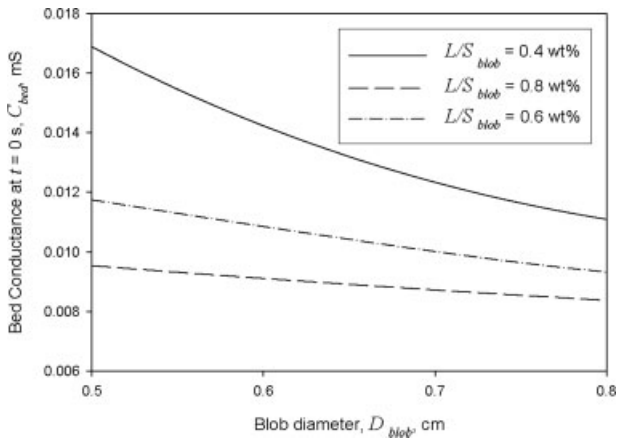

Figure 13. Predicted effect of the blob diameter D_{blob}, on the bed conductance (x_{blobs} = 84 wt %).

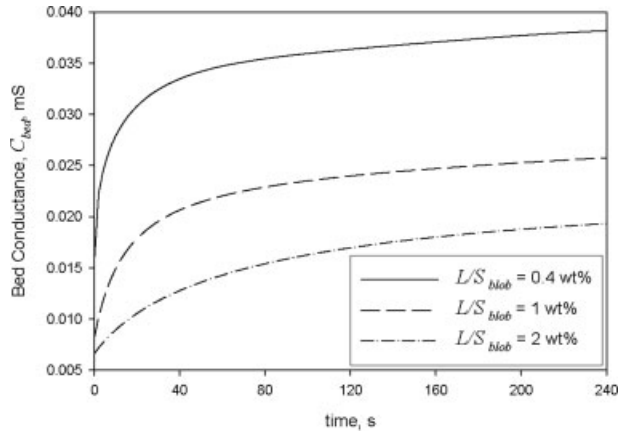

Figure 14. Predicted time evolution of the bed conductance (R_{blob} = 0.0025 m; x_{blobs} = 84 wt %).

effect of the blob size on the bed conductance becomes negligible.

Ultimately, Figure 14 shows the predicted time evolution of the bed conductance for three different values of the blob wetness, namely 0.4, 1 and 2 wt %. For all of the three cases, the fraction of liquid in blobs was 84%, and the blob diameter was 5 mm. The simulation results plotted in Figure 14 show that a more uniform initial distribution of the liquid (lower L/S_{blob}) produces a more rapid increase of the bed conductance with time. A similar effect was observed for the experimentally-determined conductance-vs.-time curves shown in Figure 5.

In conclusion, the numerical model showed that the bed electrical conductance is higher when the liquid is more uniformly spread over the solid particles. A question that still needed to be answered is to what extent changes in the liquid distribution within the bed particles as those detected by the conductance technique would have an impact on the performance of a reacting system, such as a fluid coker. In industrial fluid cokers, bitumen is injected onto preheated, steam-fluidized coke particles at temperatures ranging between 500 and 550 °C. The injected bitumen contacts the solid particles, and forms bitumen-coke agglomerates in which coke particles are bound together by liquid bridges. House et al.[11] developed a model to simulate the heat-and mass-transfer processes occurring within reacting bitumen-coke agglomerates. Their model simulates the cracking and devolatilization of bitumen in an agglomerate of given initial diameter and wetness. This allows for the prediction of the apparent kinetic rate of reaction and devolatilization for agglomerates of predefined wetness and diameter. Their work showed that reducing either the agglomerates size or wetness contributes to increasing the apparent rate of reaction and devolatilization.

Figures 12 and 13 readily show that the bed conductance technique allows capturing the effect of both these two important parameters, e.g., agglomerate size (D), and wetness (L/S). By looking more closely at Figure 13, however, it can be noticed that fairly different liquid distributions (D = 0.5 cm, with L/S = 0.8 wt %, D = 0.65 cm, with L/S = 0.6 wt %, D = 0.8 cm, with L/S = 0.4 wt %) produce nearly the same bed conductance. In order to understand whether or not these different liquid distributions are equivalent also in terms of coker performance, the same agglomerate sizes and wetness were used as input parameters to the model proposed by House et al.[11] The simulations used a composition for Athabasca vacuum residue that is consistent with the kinetic studies of Gray et al.[15] Figure 15 shows the predicted fraction of the injected liquid remaining in the agglomerate (agglomerate liquid hold up) as a function of the reaction time for agglomerate initial conditions similar to those considered in Figure 13.

Interestingly, all agglomerates react and devolatilize at approximately the same rate. For this particular set of initial conditions, the agglomerate size has no effect on the predicted rate of cracking and devolatilization, whereas decreasing the liquid-to-solid ratio results in a minimal increase in the reaction rate only over the first 1 s of the simulations. During this period, the devolatilization of both heavy and light residue dominates the kinetic behavior, and a deviation from first-order behavior is observed. Eventually, the partial pressure of the light and heavy residues saturates, and these components must react to form gas oil or distillate components for devolatilization to take place. Over the range of conditions studied, this suggests that initial liquid distributions producing a nearly identical bed conductance are also equivalent with respect to agglomerate reaction and devolatilization rate.

The apparent rate of reaction and devolatilization is important because of its influence on reactor operability. If the apparent rate of reaction and devolatilization in a fluid coker is low, the liquid holdup in the coker will be high for a given feed rate. Higher liquid holdups can result in reactor bogging and increase the propensity toward fouling of reactor internals, especially baffles (sheds) located in the stripper.[2]

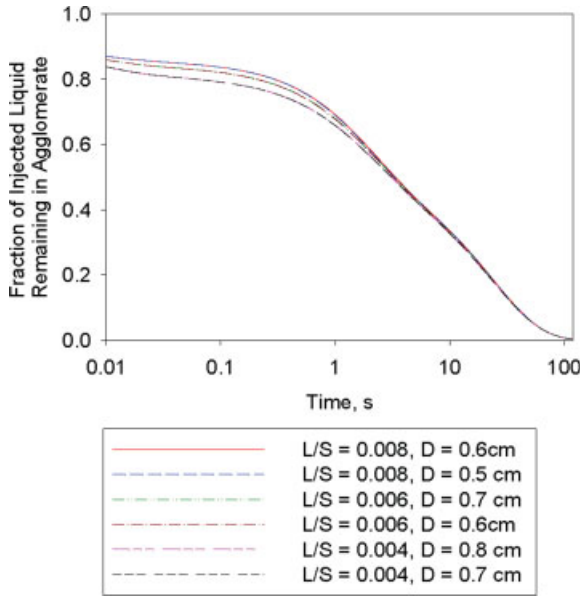

Figure 15. Predicted fraction of liquid remaining in agglomerate for different values of the agglomerate size and wetness.

[Color figure can be viewed in the online issue, which is available at www.interscience.wiley.com.]

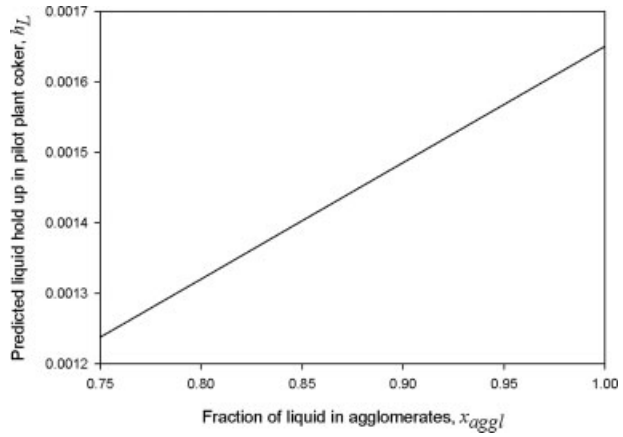

Figure 16. Predicted effect of the fraction of liquid in agglomerates (x_{aggl}) on the liquid hold-up in pilot plant coker (h_L).

Fouling of these internals has led to reduced operability and even shutdown of commercial cokers.[16] Furthermore, bogging concerns are a potential bottleneck on production rate. Therefore, it is desirable to operate with a low-liquid holdup or, equivalently, a high-apparent rate of reaction and devolatilization.

In order to predict the impact of agglomerate size and wetness on the liquid holdup in a pilot plant coker, House et al.[11] combined apparent kinetic rate equations with a CSTR model of a pilot plant coker. The simulated coker had a solids inventory of 667 kg of coke particles, and was fed at a constant rate of 5.3 kg/min of vacuum topped bitumen (VTB). The feed was considered to form agglomerates of a predefined wetness and diameter. They found that reductions in the apparent rate of cracking and devolatilization, caused by larger and wetter agglomerates, would result in higher liquid holdups in the coker. The effect of the fraction of feed forming agglomerates was not considered.To predict the effect of the fraction of the injected liquid forming agglomerates (x_{aggl}) on the performance of the pilot plant coker described in House et al.,[11] further simulations were performed combining the apparent rate of reaction and devolatilization in Figure 15, and the aforementioned CSTR model.

The feed was partitioned into two separate streams: one forming only agglomerates of predefined diameter and *L*/*S*, and one stream which coated bed particles with thin liquid films. It was assumed that the fraction of injected liquid coating particles with thin films was distributed uniformly over all the solid particles in the bed, resulting in extremely thin films. Thus, feed liquid in this phase could instantly devolatilize.

The agglomerate diameter chosen for the other stream was 0.5 cm, and its liquid-to-solid ratio was 0.4 wt %, which are the agglomerate characteristics considered in Figure 11. The results of these simulations are shown in Figure 16.

It can be seen that the predicted liquid holdup in the pilot plant coker increases with increasing fraction of liquid in agglomerates. Comparison of Figure 16 with Figure 11 shows that a larger fraction of liquid in blobs, indicated by a lower bed conductance in Figure 11, would have a detrimental effect on the performance of the coker.

Experimental results

In a previous work by the authors,[10] the quality of the jet-bed interaction was assessed using a triboelectric technique. Triboelectric measurements were conducted during the injection of liquid into the fluidized bed via gas-atomization nozzle, as well as the following mixing and drying stages, until the injected liquid had completely vaporized. In that work, the triboelectric signal recorded during the nozzle-injection of liquid and the mixing phase was normalized by the reference signal provided by an *external premixing experiment* analogous to the one described in the *Experimental* section. The resulting triboelectric nozzle performance index (TNPI) was used to rank the performance of the spray nozzle under different operating conditions, including liquid flow rate and ALR.[13]

In this study, the performance of the spray nozzle was assessed by defining a conductivity nozzle performance index (CNPI) as the ratio of the conductance measured after 10 s of defluidization for a liquid injection via nozzle to the conductance measured during the *external premixing experiment* (0.1665 mS). Using the value of the bed conductance at t = 10 s ensured that the transient effects associated with the defluidization of the bed solids had completely dissipated. A CNPI equal to 1 would correspond to liquid-solid contacting as efficient as that achieved with the *external premixing*. In practice, none of the liquid injections performed with the gas-atomization nozzle was able to provide the same coating of the solid particles with liquid as the *external premixing*, and the CNPI was always much lower than one.

Figure 17 compares the conductivity index (CNPI) to the triboeletric index (TNPI) for liquid injections carried out with the same spray nozzle and ALRs varying within the range between 0 and 3.3 wt %. It is noteworthy that the two indices varied over a similar range from a minimum of approximately 3.5% to a maximum value of 12.5% for the TNPI, and between 2 and 14% for the CNPI. Both methods, thus, indicate that the quality of the liquid-solid contact achieved by injecting liquid via a conventional spray nozzle is considerably lower than that provided by the *external premixing*. Interestingly, the CNPI exhibited a higher sensitivity

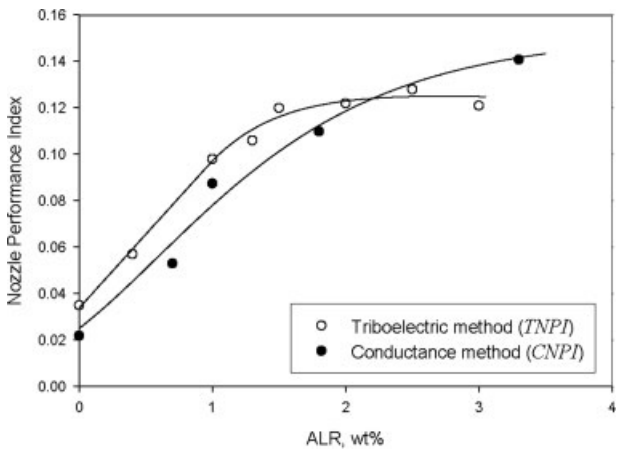

Figure 17. Effect of varying the ALR on the triboelectric nozzle performance index TNPI, and on the conductive nozzle performance index, CNPI.

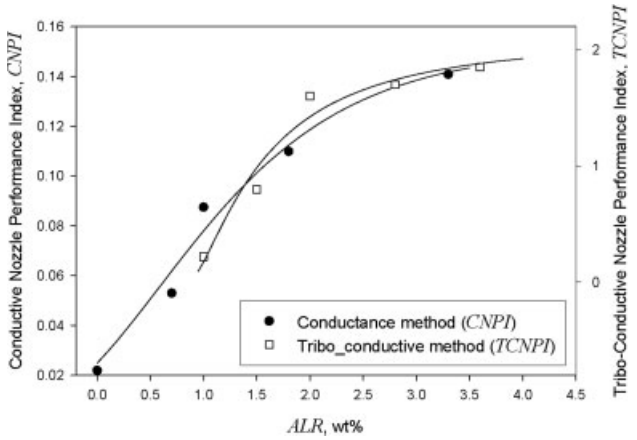

Figure 18. Effect of varying the ALR on the conductive nozzle performance index, CNPI, and on the triboconductive nozzle performance index TCNPI.

to changes in the ALR beyond 1–2 wt %. Contrary to the TNPI which plateaus for ALRs higher than 2 wt %, the CNPI consistently increases with increasing ALR. The rate of increase of the CNPI with the ALR, however, diminishes at ALRs higher than 1–2 wt %.

A very similar behavior was observed by Leach et al.[14] who assessed the nozzle performance using a third, independent experimental technique based on the injection of an electrically conductive liquid (water) into a fluidized bed of electrically insulating particles (silica sand). In that study, the dry bed particles were first tribocharged by the numerous collisions with the walls of the fluidized bed, and with a grounded electrode. To enhance particles tribocharging, high-velocity air was purged through the spray nozzle in between consecutive liquid injections. After the injection of water into the bed, the wetted solids were defluidized. The tribocharges accumulated on the solid particles could then discharge to the ground through the high-conductivity paths offered by the liquid spread on the particles. The intensity of the discharging current measured through the electrode was used as an indicator of the quality of the liquid-solid mixing, and the associated nozzle performance. Leach et al. found that the rate of increase of the nozzle performance with increasing ALR for ALRs between 1 and 2 wt % was more than double that observed at ALRs between 2 and 3.6 wt %.

A direct comparison between the conductance method and the triboconductive method is shown in Figure 18. The results obtained with the two methods were in very good agreement. The higher sensitivity displayed by the conductance and triboconductive methods is attributable to the defluidization of the bed. With the triboelectric method, the weaker agglomerates formed at high ALRs are likely to quickly breakup due to the vigorous fluidization conditions maintained after the liquid injection. Defluidizing the bed just after the end of the liquid injection, instead, preserves most of the weaker agglomerates, and, hence, allows detecting even the differences in the initial liquid-solid contact as those occurring at ALRs higher than 1–2 wt %. Despite its high-sensitivity, the triboconductive method has the drawback of requiring high tribocharging of the solid particles, which, in the study by Leach et al.[14] resulted in significant particle attrition. Particle attrition would be problematic in a large-scale fluidized bed, which makes the conductance method more suitable for scaleup studies.

The reproducibility of the conductance method was characterized by normalizing the 95% confidence intervals associated with the measured CNPI by the whole range of the index values for the five different ALRs tested. For each operating condition, six duplicate liquid injections were available. Figure 19 shows that all the normalized 95% confidence intervals calculated on the CNPI were lower or equal to 0.05. Performing the same calculations on the TNPI indicated that the reproducibility of the electrical conductance method is higher than that of the triboelectric method, which, on the average, exhibited higher values of the normalized confidence intervals over the whole ALR range explored.

Conclusions

A new experimental technique was developed to characterize the performance of gas-atomization nozzles spraying liquid into a gas-solid fluidized bed. The technique can be applied when the bed solids and the injected liquid have significantly different electrical conductivities. In this study, electrically insulating silica sand particles were wetted with deionized water, which is considerably more conductive than sand. Changes in the bed electric conductance produced by the injection of water were measured after completion of the liquid injection when the bed solids were defluidized. The extent by which the bed electric conductance increased depended on the quality of the liquid-solid mixing achieved during the injection, prior to defluidizing the bed, a more uniform distribution of the liquid over the particles resulting in a higher bed conductance. Moreover, for each case, the bed conductance increased over time due to the gradual diffusion of liquid through the packed-bed solids.

A numerical model was developed to gain further insight into the relationship existing between the measured bed elec-

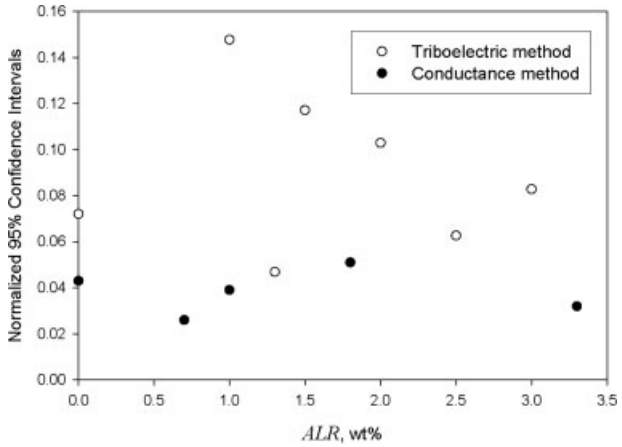

Figure 19. Reproducibility of the conductance method compared to the triboelectric method: normalized 95% confidence intervals calculated on CNPI and TNPI for different ALRs.

tric conductance and the liquid-solid contacting efficiency of the liquid injection into the fluidized bed. The model was used to investigate the effects of several parameters characterizing the uniformity of the liquid-solid mixture on the bed electric conductance. The numerical study indicated that a higher degree of homogeneity of the liquid-solid mixture obtained by reducing the fraction of liquid forming liquid-solid agglomerates, the wetness of the agglomerates formed, or the agglomerate size results in a higher bed conductance. Furthermore, the reaction model developed by House et al.[11] was used to simulate the impact that changes in each of these three parameters, e.g., fraction of liquid in agglomerates, agglomerate wetness, and agglomerate size, would have on the performance of a pilot plant fluid coker. The simulations indicated that a higher uniformity of the liquid-solid distribution as assessed by the conductance technique would result in a higher performance of the coker.

The experimental method was applied to studying the effect of the air-to-liquid ratio (ALR) on the performance of a nozzle spraying liquid into the fluidized bed. A nozzle performance index (CNPI) was defined based on the bed electric conductance measured after completion of the liquid injection and bed defluidization. Increasing the ALR was beneficial to the nozzle performance over the whole range of ALRs tested (0–3.3 wt %). However, this effect was more pronounced at low ALRs, up to 1–2 wt %. Comparison of the *CNPI* with nozzle performance indices derived from different experimental techniques indicated that the electric conductance method is both highly sensitive to changes in the nozzle operating conditions and reproducible. As an additional advantage, the method can be easily implemented in larger-scale fluidized beds.

Acknowledgments

The authors greatfully acknowledge financial support from Syncrude Canada and from the Natural Sciences and Engineering Council of Canada. The authors would also like to thank Professor Ion Inculet, of the Department of Electrical and Computer Engineering of the University of Western Ontario, for his advice and help.

Notation

ALR = air-to-liquid ratio, wt %
c = water concentration, mol/m^3
C_{bed} = bed electrical conductance, S
C_{box} = box electrical conductance, S
$CNPI$ = nozzle performance index based on the electrical conductance method
D = diffusion coefficient, m^2/s
D_{blob} = blob diameter, cm
E = electric field, V/m
f_{segr} = ratio of the liquid segregated in the blobs to the total mass of solids, wt %
f_{free} = ratio of the liquid outside of the blobs to the total mass of solids, wt %
F_g = geometrical constant
G = geometrical factor, m
I = electric current, A
h_L = liquid holdup in pilot plant coker
J = electric current density, A/m^2
L/S_{blob} = liquid-to-solid weight ratio in each blob, wt %
L/S_{total} = liquid-to-solid weight ratio in the entire domain, wt %
M_{Lblob} = mass of liquid in each blob, Kg
t = elapsed time after bed defluidization, s
$TNPI$ = nozzle performance index based on the triboelectric method
V = electric potential, V
V_{Lblob} = volume occupied by the liquid phase in a blob, m^3
V_{Sblob} = volume occupied by the solid phase in a blob, m^3
V_{ref} = reference electric potential, V
V_1 = voltage produced by the signal generator, V
V_2 = voltage measured across the resistor R_m, V
V_g = superficial gas velocity, m/s
x_{aggl} = fraction of liquid segregated in agglomerates
x_{blobs} = fraction of liquid segregated in blobs, %

Greek letters

σ = electric conductivity, S/m
ρ_L = liquid density, kg/m^3
ρ_S = solids density, kg/m^3

Literature Cited

1. House PK, Saberian M, Briens C, Berruti F, Chan E. Injection of a liquid spray into a fluidized bed: particle-liquid mixing and impact on fluid coker yields. *Ind Eng Chem Res*. 2003;43:5663–5669.
2. House P, Berruti F, Gray M, Chan E, Briens C. *Prediction of Propensity to Fouling in Fluid Cokers*. AIChE National Meeting, San Francisco; November 12–17, 2006.
3. Gray M. *Upgrading of petroleum residues and heavy oils*. New York: Marcel Dekker, Inc; 1994.
4. Leclere K, Briens C, Gauthier T, Bayle J, Bergougnou M, Guigon P. Liquid vaporization in a fluidized bed. *Ind Eng Chem Res*. 2001; 40:5415–5420.
5. Leclere K, Briens C, Gauthier T, Bayle J, Guigon P, Bergougnou M. Experimental measurement of droplet vaporization kinetics in a fluidized bed. *Chem Eng Proc*. 2004;43:693–699.
6. Ariyapadi S, Holdsworth D, Norley C, Berruti F, Briens C. Digital X-ray imaging technique to study the horizontal injection of gas-liquid jets into fluidized beds. *Int J Chem React Eng*. 2003;1:A56.
7. Bruhns S, Werther J. An investigation of the mechanism of liquid injection into fluidized beds. *AIChE J*. 2005;51:766–775.
8. House P, Briens C, Berruti F, Chan E. Injection of a liquid spray into a fluidized bed: enhancing particle-liquid mixing. *Powder Technol*. 2007; in press.
9. Knapper BA, Gray MR, Chan EW, Mikula R. Measurement of efficiency of distribution of liquid feed in a gas-solid fluidized bed reactor. *Int J Chem React Eng*. 2003;1:A35.
10. Portoghese F, Berruti F, Briens C, Chan E. Novel triboelectric method for characterizing the performance of nozzles injecting gas-atomized liquid into a fluidized bed. *Chem Eng Proc*. 2008;46:924–934.
11. House PK, Briens C, Berruti F. Thermal cracking of bitumen in an agglomerate. *Chem Eng Sci*. 2007; submitted.
12. Chan EW, Base TE, Kennett RD, Emberley DA, Jonasson K, McCracken TW, Bennett AJ, CA Patent 2224615; 1997.
13. Portoghese F, Ferrante L, Berruti F, Briens C, Chan E. Effect of injection-nozzle operating parameters on the interaction between a gas-liquid jet and a gas-solid fluidized bed. *Powder Technol*. 2008;184:1–10.
14. Leach A, Portoghese F, Briens C, Berruti F. New, rapid method for the evaluation of the liquid-solid contact resulting from liquid injection into a fluidized bed. *Powder Technol*. 2008;184:44–51.
15. Gray M, McCaffrey MC, Huq I, Le T. Kinetics of cracking and devolatilization during coking of athabasca residues. *Ind Eng Chem Res*. 2004;43:5438–5445.
16. Bi HT, Grace JR, Lim CJ, Rusnell D, Bulbuc D, McKnight CA. Hydrodynamics of the stripper section of fluid cokers. *Can J Chem Eng*. 2005;83:161–168.

Manuscript received Sept. 5, 2007, and revision received Feb. 24, 2008.